

Techni-dilaton signatures at LHC

Shinya Matsuzaki^{1,*} and Koichi Yamawaki^{2,†}

¹ *Maskawa Institute for Science and Culture, Kyoto Sangyo University,
Motoyama, Kamigamo, Kita-Ku, Kyoto 603-8555, Japan.*

² *Kobayashi-Maskawa Institute for the Origin of Particles and the Universe (KMI)
Nagoya University, Nagoya 464-8602, Japan.*

(Dated: April 3, 2024)

We explore discovery signatures of techni-dilaton (TD) at LHC. The TD was predicted long ago as a composite pseudo Nambu-Goldstone boson (pNGB) associated with the spontaneous breaking of the approximate scale symmetry in the walking technicolor (WTC) (initially dubbed “scale-invariant technicolor”). Being pNGB, whose mass arises from the explicit scale-symmetry breaking due to the spontaneous breaking itself (dynamical mass generation), the TD as a composite scalar should have a mass M_{TD} lighter than other techni-hadrons, say $M_{\text{TD}} \simeq 600$ GeV for the typical WTC model, which is well in the discovery range of the ongoing LHC experiment. We develop a spurion method of nonlinear realization to calculate the TD couplings to the standard model (SM) particles and explicitly evaluate the TD LHC production cross sections at $\sqrt{s} = 7$ TeV times the branching ratios in terms of M_{TD} as an input parameter for the region $200 \text{ GeV} < M_{\text{TD}} < 1000 \text{ GeV}$ in the typical WTC models. It turns out that the TD signatures are quite different from those of the SM Higgs: In the one-doublet model (1DM) all the cross sections including the WW/ZZ mode are suppressed compared to those of the SM Higgs due to the suppressed TD couplings, while in the one-family model (1FM) all those cross sections get highly enhanced because of the presence of extra colored fermion (techni-quark) contributions. We compare the $\text{TD} \rightarrow WW/ZZ$ signature with the recent ATLAS and CMS bounds and find that in the case of 1DM the signature is consistent over the whole mass range $200 \text{ GeV} < M_{\text{TD}} < 1000 \text{ GeV}$ due to the large suppression of TD couplings, and by the same token the signal is too tiny for the TD to be visible through this channel at LHC. As for the 1FMs, on the other hand, a severe constraint is given on the TD mass to exclude the TD with mass $\lesssim 600$ GeV, which, however, would imply an emergence of somewhat dramatic excess as the TD signature at $600 \text{ GeV} \lesssim M_{\text{TD}} < 1000 \text{ GeV}$ in the near future. We further find a characteristic signature coming from the $\gamma\gamma$ mode in the 1FM. In sharp contrast to the SM Higgs case, it provides highly enhanced cross section $\sim 0.10\text{--}1.0$ fb at around the TD mass $\simeq 600$ GeV, which is large enough to be discovered during the first few years’ run at LHC.

I. INTRODUCTION

Large Hadron Collider (LHC) has started setting the strong constraints on the standard model (SM) Higgs boson, the key particle responsible for the origin of mass in the context of the SM. The recent data from the ATLAS [1] and CMS [2] experiments suggest that the SM Higgs boson is unlikely for the mass range as low as the electroweak (EW) scale, which may suggest that there might exist certain composite dynamics for the origin of mass due to the strongly coupled theories like technicolor (TC) [3]. Actually, in contrast to the original TC [4], a Higgs-like object, techni-dilaton (TD), was predicted as a composite scalar, a pseudo Nambu-Goldstone boson (pNGB) associated with the spontaneously broken approximate scale symmetry in the walking TC (WTC), initially dubbed “scale-invariant TC” [5, 6]. Thus clarifying the TD signature at LHC is the urgent task in searching for Higgs-like particle at the ongoing LHC, which is the target of this paper.

The original version of TC [4], a naive scale-up version of QCD, was dead due to the excessive flavor-changing neutral currents (FCNC). A solution to the FCNC problem was soon suggested by simply assuming the existence of a large anomalous dimension without any concrete dynamics and concrete value of the anomalous dimension [7]. It was the WTC [5, 6] that gave a concrete dynamics, ladder Schwinger-Dyson (LSD) equation with *non-running* (scale invariant/conformal) gauge coupling, $\alpha(p) \equiv \alpha$, giving rise to a concrete value of the anomalous dimension, $\gamma_m = 1$ at criticality $\alpha = \alpha_c$. Actually, once the mass m_F of the techni-fermion (F) is dynamically generated, the coupling becomes *running slowly* (“walking”) a la Miransky [8], with the *nonperturbative* beta function $\beta(\alpha) \sim$

*synya@cc.kyoto-su.ac.jp

†yamawaki@kmi.nagoya-u.ac.jp

$-(\alpha/\alpha_c - 1)^{3/2}$ ($\alpha > \alpha_c$). (Subsequently, a similar FCNC solution based on the (*perturbatively*) walking coupling was discussed without concept of anomalous dimension [9].) ^{#1}

In view of the approximate scale symmetry reflected by the *nonperturbative* walking coupling associated with the dynamical generation of m_F , the WTC predicted the TD [5, 6], a light scalar $\bar{F}F$ composite as a pNGB associated with the spontaneous breaking of the approximate scale symmetry triggered by the dynamical generation of m_F or the techni-fermion condensate. This is in sharp contrast to the TC as a simple scale-up of the QCD where the coupling is *running already at perturbative level* with the scale symmetry badly broken at Λ_{QCD} , so that there is no scale symmetry to be broken by the dynamical fermion mass generation and hence no scalar spectrum lighter than the typical hadronic scale, say the rho meson ^{#2}. The mass generation due to such a scale invariant (conformal) dynamics takes the form of essential-singularity scaling, Miransky scaling [8], and can be characterized by the “*conformal phase transition*” [15].

It should be noted here that even if the gauge coupling is non-running (scale invariant) in the *perturbative* sense as in the case of the LSD equation, the scale symmetry is actually *broken explicitly for the very reason of the spontaneous breaking itself*, namely the dynamical generation of the techni-fermion mass m_F , which is responsible for the *nonperturbative* running of the coupling (*nonperturbative* scale anomaly) as mentioned above. Accordingly, the TD cannot be massless even if we use a *perturbatively* non-running (scale invariant) coupling in the LSD equation. Actually, various old calculations [16, 17] imply $M_{\text{TD}} = \mathcal{O}(m_F)$, still smaller, though not extremely smaller, than masses of other techni-hadrons.

Modern version of WTC [15, 18, 19] is based on the two-loop running coupling with the Caswell-Banks-Zaks infrared fixed point (CBZ-IRFP) [20], instead of the non-running one, in the improved LSD equation. There also exists an intrinsic scale Λ_{TC} analogous to Λ_{QCD} , which breaks the scale symmetry already at two-loop perturbative level for the ultraviolet region $p > \Lambda_{\text{TC}}$ (taken to be $> \Lambda_{\text{ETC}} > 10^3$ TeV) where the coupling runs in the same way as in QCD. However this *perturbative* scale-symmetry-breaking scale Λ_{TC} is irrelevant to the dynamical mass m_F and so is the TD mass M_{TD} , both can be $\ll \Lambda_{\text{TC}}$ thanks to the CBZ-IRFP.

Indeed, it has recently been argued [21, 22] and explicitly shown [23] in the case of the two-loop perturbative coupling that we have essentially the same conclusion as the non-running case in the above, $M_{\text{TD}} = \mathcal{O}(m_F) (\ll \Lambda_{\text{TC}})$, in sharp contrast to the recent claim on much smaller mass $M_{\text{TD}} \ll \mathcal{O}(m_F)$ [24] ^{#3}. Namely, the dynamical generation of m_F triggers spontaneous breaking of the scale symmetry which is also *explicitly broken by m_F* through the *nonperturbative running* coupling (*nonperturbative scale anomaly*) again a la Miransky. At any rate the approximate scale symmetry is crucial for the mass of TD to be lighter than other techni-hadrons like techni-rho meson with the mass M_ρ , ($\Lambda_{\text{TC}} \gg M_\rho > \mathcal{O}(\text{TeV}) > M_{\text{TD}} = \mathcal{O}(m_F)$). More concretely, it was noted [21] that several earlier nonperturbative calculations of the scalar mass in different contexts can be interpreted as those for the estimate of TD mass [27, 28]: $M_{\text{TD}} \simeq \sqrt{2}m_F$, which would suggest the TD mass as low as

$$M_{\text{TD}} \simeq 600 \text{ GeV} \quad (1)$$

(one-family model), well within the reach of LHC searches. This is also consistent with the recent holographic estimate [25] and others [29]. (The above estimate would suggest $M_{\text{TD}} \simeq 1$ TeV for the one-doublet model, barely within the LHC search region) ^{#4}.

In this paper, we explore the characteristic signature of TD at the LHC, calculating the relevant decay widths and production cross sections in comparison with those of the SM Higgs. To set definite benchmarks, we employ typical models of TC [3] such as the one-doublet model (1DM) ^{#5} and one-family model (1FM) in the light of WTC.

^{#1} Another problem of the TC as a QCD scale-up is the electroweak constraints, so-called S, T, U parameters. This may also be improved in the WTC [10, 11]. Even if WTC in isolation cannot overcome this problem, there still exist a possibility that the problem may be resolved in the combined dynamical system including the SM fermion mass generation such as the extended TC (ETC) dynamics [12], in much the same way as the solution (“ideal fermion delocalization”) [13] in the Higgsless models which simultaneously adjust S and T parameters by incorporating the SM fermion mass profile.

^{#2} There might exist a light scalar, so-called σ resonance, in the real-life QCD, which however may not be a two-body composite of $\bar{q}q$ which is an analogue of TD but may be mainly a four-body composite. Such a situation of the real-life QCD is an accidental consequence of specific values $N_c = N_f = 3$ and $m_u \simeq m_d \ll m_s$. See e.g., [14].

^{#3} We here exclude the “decoupled TD” scenario [23, 25] with the Yukawa coupling $\sim m_F/F_{\text{TD}} \rightarrow 0$ as $m_F/\Lambda_{\text{TC}} \rightarrow 0$, which is irrelevant to LHC experiments, although it might be relevant to dark matter [23, 26].

^{#4} The TD with such a mass region gives substantial negative logarithmic contribution to the T parameter in a manner similar to the SM heavy Higgs. This could be an extra bonus, since it can in principle be compensated by the troublesome positive contributions from the techni-fermion dynamics [30].

^{#5} The 1DM in the usual sense is not walking. We here use “1DM” as a modified model (“partially gauged model”) [31] which, besides one doublet techni-fermions with EW charges as in the usual 1DM, has dummy techni-fermions without EW charges which only contribute to the walking behavior of TC dynamics. Actually, such dummy techni-fermions are needed even for 1FM with $N_{\text{TC}} = 3$ since in this

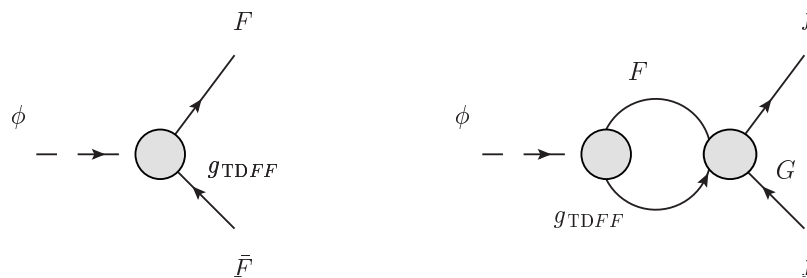


FIG. 1: The TD Yukawa couplings $g_{\text{TD}FF}$ (left panel) and $g_{\text{TD}ff}$ (right panel) to techni-fermions (F) and SM fermions (f). The blob denoted as G in the right panel corresponds to an ETC-induced four fermi vertex $G\bar{F}Fff$.

The TD couplings to the SM particles are derived based on nonlinear realization of both scale and chiral symmetries, which becomes highly nontrivial since the scale symmetry, in contrast to the chiral symmetry, is broken explicitly as well as spontaneously due to the dynamical mass generation of the techni-fermion m_F , leading to the nonperturbative scale anomaly as mentioned above. There is no limit where TD becomes exactly massless. Thus the nonlinear realization of the scale symmetry must properly include the explicit breaking at the same time as the spontaneous breaking, which we will do via spurion field method, the method familiar in the chiral perturbation theory incorporating the current quark mass term [32]. Then the TD couplings are given as functions of the techni-fermion mass m_F , the TD decay constant F_{TD} (or TD Yukawa coupling) and the TD mass M_{TD} up to the number of TC N_{TC} . Note that F_{TD} may be written in terms of M_{TD} and m_F through the partially conserved dilatation current (PCDC) for the trace anomaly (nonperturbative scale anomaly) reflecting the spontaneous and explicit breaking of the scale symmetry due to dynamical generation of m_F , and m_F may be written in terms of the weak scale $v_{\text{EW}} = 246 \text{ GeV}$ through the Pagels-Stokar (PS) formula [33]. Hence we can estimate all the quantities only in terms of the TD mass M_{TD} as a free parameter which we take in a wide region $200 \text{ GeV} < M_{\text{TD}} < 1000 \text{ GeV}$ around the reference value 600 GeV in Eq.(1) suggested by the various calculations [21, 25]. In order to do a concrete estimate we adopt a recent result of the nonperturbative scale anomaly [23] based on the LSD analysis with the two-loop beta function of large N_f QCD having the CBZ-IRFP [20]. The result is not qualitatively changed (see the discussion in the last section) if we employ the non-running coupling in the LSD as in Refs. [5, 6].

We then explicitly evaluate the LHC production cross sections of TD at $\sqrt{s} = 7 \text{ TeV}$, σ_{TD} , times the TD branching ratios, for the TD mass range taken within the LHC search region $200 \text{ GeV} < M_{\text{TD}} < 1000 \text{ GeV}$. We find that the TD signatures are quite different from those of the SM Higgs: For 1DMs all those cross sections get suppressed compared to the corresponding quantities for the SM Higgs due to the suppression of the gluon fusion cross section coming from the large suppression of TD couplings, while for 1FMs they get highly enhanced since the production cross section has huge extra contributions from the extra colored fermions (techni-quarks). As a check of consistency with the current LHC data, we compare the cross section $\sigma_{\text{TD}} \times BR(\text{TD} \rightarrow WW)$ normalized to the corresponding quantity for the SM Higgs with the recent bounds from the ATLAS [1] and CMS [2] experiments ^{#6}. It turns out that in the case of 1DMs the signature is consistent with the current experimental data over the whole region we study thanks to the large suppression of TD couplings, and by the same token the signal is too tiny to be visible through this channel at LHC. As for the 1FMs, on the other hand, the TD mass is constrained to be excluded up till $M_{\text{TD}} \simeq 600 \text{ GeV}$, which, however, would imply occurrence of somewhat large excess at $600 \text{ GeV} \lesssim M_{\text{TD}} < 1000 \text{ GeV}$ in this channel to be seen in the future experiments. We further calculate the cross section $\sigma_{\text{TD}} \times BR(\text{TD} \rightarrow \gamma\gamma)$ and predict it to be $\sim 0.10 - 1.0 \text{ fb}$ at $\sqrt{s} = 7 \text{ TeV}$ for the TD mass around 600 GeV in the typical 1FMs. This cross section is comparable with the golden mode of the SM Higgs $pp \rightarrow h_{\text{SM}} \rightarrow ZZ \rightarrow l^+l^-l^+l^-$, and hence is large enough for the TD to be discovered within the first few year's run at the LHC.

case $N_{\text{TF}} = 4N_{\text{TC}} = 12 > 8$.

^{#6} As far as the current Higgs research mass region up to 600 GeV is concerned, the narrow width approximation can be applied to TD even in the 1FMs as well as the SM Higgs, since the TD with mass up to 600 GeV turns out to have an almost identical size of total width compared to the SM Higgs. The narrow width approximation is much better in the case of 1DMs which have highly suppressed couplings.

II. THE TD COUPLINGS AND DECAY WIDTHS

In this section we shall derive the TD couplings to the SM particles and address their forms. We focus on the couplings to $WW, ZZ, gg, \gamma\gamma$ and $t\bar{t}$ to make the explicit comparison with those of the SM Higgs.

The TD Yukawa couplings to the techni-fermion $g_{\text{TD}FF}$ and those to the SM fermions $g_{\text{TD}ff}$ were actually derived long time ago [6] through the Ward-Takahashi identity for dilatation current coupled with TD, corresponding to the diagrams depicted in Fig. 1:

$$g_{\text{TD}FF} = \frac{(3 - \gamma_m)m_F}{F_{\text{TD}}}, \quad g_{\text{TD}ff} = \frac{(3 - \gamma_m)m_f}{F_{\text{TD}}}, \quad (2)$$

where $(3 - \gamma_m)$ denotes the scale dimension of techni-fermion bilinear operator $\bar{F}F$, which is $\simeq 2$ for the anomalous dimension $\gamma_m \simeq 1$ in WTC and we have assumed an ETC-induced four-fermi interaction such as $G\bar{F}Fff$ which gives the f -fermion mass $m_f = -G\langle\bar{F}F\rangle$ ^{#7}.

Here we work on nonlinear realization of both the scale and chiral symmetries to derive a nonlinear Lagrangian which directly yields the various TD couplings to the SM particles. Actually, the resultant Lagrangian *should not be invariant* under the scale symmetry because it is broken by techni-fermion mass generation explicitly as well as spontaneously as was emphasized above. We therefore incorporate such an inherent explicit-breaking effects (nonperturbative scale anomaly) arising from the dynamical mass generation itself by introducing a spurion field in a familiar manner [32], which will provide us with a direct way to read appropriate couplings of TD.

We begin by introducing a dynamical variable Φ which reflects the scale transformation property of the techni-fermion bilinear $\bar{F}F$ ($\Phi \approx \frac{\bar{F}F}{\langle\bar{F}F\rangle}$), analogously to the usual chiral field U reflecting the chiral transformation property of $\bar{q}_L q_R$, so that Φ transforms under the scale symmetry as

$$\delta\Phi = (3 - \gamma_m + x^\nu \partial_\nu) \Phi. \quad (3)$$

We parametrize this Φ with the TD field ϕ and the decay constant F_{TD} as

$$\Phi = e^{(3-\gamma_m)\phi/F_{\text{TD}}}, \quad (4)$$

where F_{TD} is defined as

$$\langle 0 | D_\mu(0) | \phi(p) \rangle = -ip_\mu F_{\text{TD}}, \quad (5)$$

with D_μ being the dilatation current composed *only of the TC sector fields*. From Eq.(3) it follows that the TD field ϕ transforms nonlinearly under the scale symmetry:

$$\delta\phi = F_{\text{TD}} + x^\nu \partial_\nu \phi. \quad (6)$$

To incorporate the explicit-breaking effects due to the nonperturbative scale anomaly of the TC sector, we introduce a spurion field S which transforms under the scale symmetry with the scale dimension 1:

$$\delta S = (1 + x^\nu \partial_\nu) S. \quad (7)$$

Its vacuum expectation value $\langle S \rangle = 1$ thus breaks the scale symmetry explicitly.

We further introduce the usual chiral field $U = e^{2i\pi/v_{\text{EW}}}$, with π being the NGB fields for the spontaneous chiral symmetry breaking, and consider only the would-be NGBs eaten by W and Z bosons for simplicity ^{#8}. This U and π should have scale dimension 0 such that π transform linearly under the scale symmetry.

With these at hand, we can write down a nonlinear Lagrangian *invariant* under the EW and scale symmetries *including the spurion field S* . The Lagrangian is constructed so as to reproduce the appropriate scale anomaly terms coupled to TD generated in the underlying WTC when $\langle S \rangle = 1$ is taken. It turns out that the Lagrangian including

^{#7} The top mass is hardly reproduced by the WTC with anomalous dimension $\gamma_m \simeq 1$. It may require other dynamics such as the top quark condensate [34]. However, it was found [35] that if we include additional four-fermion interactions like strong ETC, the anomalous dimension becomes much larger $1 < \gamma_m < 2$, which can boost the ETC-origin mass to arbitrarily large up till the techni-fermion mass scale ("strong ETC model"). Subsequently the same effects were also noted without concept of the anomalous dimension [36].

^{#8} Here we have ignored terms involving techni-pions not eaten by W and Z bosons which would appear in models such as 1FM. Even if we incorporate them, however, the forms of TD couplings to the SM particles given here will be intact.

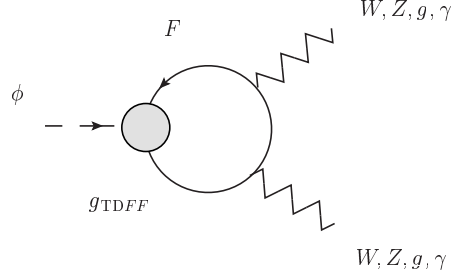


FIG. 2: The TD couplings to $WW, ZZ, gg, \gamma\gamma$ induced from techni-fermion loops.

the TD couplings to the SM particles at the leading order takes the form ^{#9} (The explicit proof of the Wess-Zumino type consistency with the scale anomaly is to be given in another publication.)

$$\begin{aligned} \mathcal{L} = & \frac{v_{\text{EW}}^2}{4} (\Phi S^{\gamma_m-2})^2 \text{tr}[D_\mu U^\dagger D^\mu U] - (\Phi S^{\gamma_m-2}) \sum_f \left(\bar{f}_L U \begin{pmatrix} m_f^u & 0 \\ 0 & m_f^d \end{pmatrix} f_R + \text{h.c.} \right) \\ & - (\Phi S^{\gamma_m-3}) \left(\frac{\beta_F(\alpha_s)}{2\alpha_s} \text{tr}[G_{\mu\nu}^2] + \frac{\beta_F(\alpha_{\text{EM}})}{4\alpha_{\text{EM}}} F_{\mu\nu}^2 \right), \end{aligned} \quad (8)$$

where $D_\mu U = \partial_\mu U - ig_W W_\mu^a \frac{\sigma^a}{2} U + ig_Y U B_\mu \frac{\sigma^3}{2}$; W_μ^a ($a = 1, 2, 3$) and B_μ are the $SU(2)_W$ and $U(1)_Y$ gauge fields with the gauge couplings g_W and g_Y ; σ^a denotes Pauli matrices; $G_{\mu\nu}$ and $F_{\mu\nu}$ are field strengths for the QCD gluon and electromagnetic (EM) gauge (photon) fields with the gauge couplings $\alpha_{s,\text{EM}} = g_{s,\text{EM}}^2/(4\pi)$, respectively; β_F denotes beta function including only the techni-fermion loop contributions; $f_{L,R} = (f_{L,R}^u, f_{L,R}^d)^T$ stand for the $SU(2)_{L,R}$ doublets with $m_f^{u,d}$ being their masses. Note that $\beta_F(\alpha_s) = 0$ in the case of 1DM, while $\beta_F(\alpha_{\text{EM}}) \neq 0$ because of the presence of techni-fermions having the EM charges.

Taking $\langle S \rangle = 1$, from Eq.(8) we readily find the TD couplings to WW, ZZ and $\bar{f}f$:

$$\mathcal{L}_{\text{TD}WW/ZZ} = g_{\text{TD}WW} \phi W_\mu^+ W^{\mu-} + \frac{1}{2} g_{\text{TD}ZZ} \phi Z_\mu Z^\mu, \quad (9)$$

$$\mathcal{L}_{\text{TD}ff} = -g_{\text{TD}ff} \phi \bar{f} f, \quad (10)$$

$$g_{\text{TD}WW/ZZ} = \frac{2(3 - \gamma_m)m_{W/Z}^2}{F_{\text{TD}}}, \quad g_{\text{TD}ff} = \frac{(3 - \gamma_m)m_f}{F_{\text{TD}}}, \quad (11)$$

and the couplings to gg and $\gamma\gamma$,

$$\mathcal{L}_{\text{TD}gg/\gamma\gamma} = -g_{\text{TD}gg} \phi \text{tr}[G_{\mu\nu}^2] - g_{\text{TD}\gamma\gamma} \phi F_{\mu\nu}^2, \quad (12)$$

$$g_{\text{TD}gg} = \frac{(3 - \gamma_m)}{F_{\text{TD}}} \frac{\beta_F(\alpha_s)}{2\alpha_s}, \quad g_{\text{TD}\gamma\gamma} = \frac{(3 - \gamma_m)}{F_{\text{TD}}} \frac{\beta_F(\alpha_{\text{EM}})}{4\alpha_{\text{EM}}}. \quad (13)$$

The same couplings as the above can actually be obtained by directly evaluating diagrams in Fig. 2 and the right panel of Fig. 1, hence the results for $g_{\text{TD}ff}$ and $g_{\text{TD}WW/ZZ}$ are identical to Eq.(2) and that of Ref. [38], respectively.

The couplings in Eqs.(11) and (13) are compared with the SM Higgs couplings $g_{\text{TD}WW/ZZ} = \frac{2m_{W/Z}^2}{v_{\text{EW}}}$, $g_{\text{TD}ff} = \frac{m_f}{v_{\text{EW}}}$, $g_{h_{\text{SM}}gg} = \frac{1}{v_{\text{EW}}} \frac{\beta(\alpha_s)}{2\alpha_s}$, and $g_{h_{\text{SM}}\gamma\gamma} = \frac{1}{v_{\text{EW}}} \frac{\beta(\alpha_{\text{EM}})}{4\alpha_{\text{EM}}}$, which indeed implies a simple replacement, $1/v_{\text{EW}} \rightarrow (3 - \gamma_m)/F_{\text{TD}}$ ($\simeq 2/F_{\text{TD}}$ for $\gamma_m \simeq 1$), between the SM Higgs and TD couplings. (Note that $1/v_{\text{EW}} \neq (3 - \gamma_m)/F_{\text{TD}}$, with the value of F_{TD} being related to v_{EW} in a highly model dependent way.) The essential discrepancy in coupling forms thus arises only as the overall coupling strengths set by the TD decay constant F_{TD} , in place of the EW scale $v_{\text{EW}} \simeq 246$ GeV.

Once the TD couplings are obtained, we can calculate the TD decay widths $\Gamma(\text{TD} \rightarrow X)$ ($X = WW, ZZ, gg, \gamma\gamma, t\bar{t}$) evaluating the amplitudes at the leading order of perturbation. Actually, the gg and $\gamma\gamma$ couplings in Eq.(13) are

^{#9} In Ref. [37] a similar nonlinear realization was discussed, but it does not take account of those inherent explicit-breaking effects arising from the dynamical mass generation. Note that the scale-transformation property of $(\Phi S^{\gamma_m-2}) \sim e^{\phi/F_{\text{TD}}}$, which is the same as the nonlinear base used in Ref. [37] unless taking $\langle S \rangle = 1$.

not sufficient for evaluating the $\text{TD} \rightarrow gg$ and $\gamma\gamma$ decays since these terms arise as higher dimensional (derivative) operators more sensitive to ultraviolet contributions of $\mathcal{O}(m_F)$ than the $\text{TD}-WW, ZZ$ and $t\bar{t}$ coupling terms in Eq.(11) which are of the lowest order. Therefore we shall straightforwardly evaluate techni-fermion loop contributions to the $\text{TD} \rightarrow gg$ and $\gamma\gamma$ decay widths, instead of using the operator coupling forms in Eq.(13).

We assume that all the techni-fermions belong to the fundamental representation in the TC gauge group of $SU(N_{\text{TC}})$ and have the flavor-independent mass m_F defined as usual $\Sigma(p = m_F) = m_F$ in the LSD equation analysis, where $\Sigma(p)$ is the mass function of the techni-fermions. Here we use the constant mass function $\Sigma(p) \equiv m_F$ for calculating the amplitudes for simplicity. Even if we use the momentum-dependent mass function (solution of the LSD) throughout all the calculations, the result will not be changed as far as the LHC energy $p \lesssim m_F < \mathcal{O}(\text{TeV})$ is concerned. Also used is the TD Yukawa coupling to techni-fermions $g_{\text{TD}FF}$ given in Eq.(2).

We further add the SM loop contributions to the decay widths $\Gamma(\text{TD} \rightarrow gg)$ and $\Gamma(\text{TD} \rightarrow \gamma\gamma)$, which will be relevant in magnitude as in the case of the SM Higgs, although those are of subleading order in terms of TC dynamics.

The decay widths are thus calculated to be

$$\Gamma(\text{TD} \rightarrow gg) = \frac{\alpha_s^2 M_{\text{TD}}^3}{8\pi^3 F_{\text{TD}}^2} \left| \sum_{f=t,b} \tau_f [1 + (1 - \tau_f) f(\tau_f)] + N_{\text{TC}} \sum_{F \text{ with QCD color}} \tau_F [1 + (1 - \tau_F) f(\tau_F)] \right|^2, \quad (14)$$

$$\Gamma(\text{TD} \rightarrow \gamma\gamma) = \frac{\alpha_{\text{EM}}^2 M_{\text{TD}}^3}{64\pi^3 F_{\text{TD}}^2} \left| A_W(\tau_W) + 3 \sum_{f=t,b} Q_f^2 A_f(\tau_f) + N_{\text{TC}} \sum_F N_c^{(F)} Q_F^2 A_F(\tau_F) \right|^2, \quad (15)$$

where $\tau_i = 4m_i^2/M_{\text{TD}}^2$ ($i = W, Z, f, F$); $N_c^{(F)} = 3(1)$ for techni-quarks (leptons); $Q_{f(F)}$ denotes EM charge for $f(F)$ -fermion, and

$$A_W(\tau_W) = -2[2 + 3\tau_W + 3\tau_W(2 - \tau_W)f(\tau_W)], \quad (16)$$

$$A_{f(F)}(\tau_{f(F)}) = 2\tau_{f(F)} [1 + (1 - \tau_{f(F)}) f(\tau_{f(F)})], \quad (17)$$

$$f(\tau_i) = \begin{cases} \left(\sin^{-1} \frac{1}{\sqrt{\tau_i}} \right)^2 & \text{for } \tau_i > 1 \\ -\frac{1}{4} \left[\log \left(\frac{1 + \sqrt{1 + \tau_i}}{1 - \sqrt{1 - \tau_i}} \right) - i\pi \right] & \text{for } \tau_i \leq 1 \end{cases}.$$

The $\text{TD} \rightarrow gg$ and $\gamma\gamma$ decay widths are thus quite sensitive to type of models of WTC, which leads to characteristic signatures of TD highly model-dependent, as will be seen later.

As for the formulas for $\Gamma(\text{TD} \rightarrow WW/ZZ/t\bar{t})$, it turns out that the resultant expressions for those decay widths actually take the same forms as the familiar ones for the SM Higgs, say, as listed in Ref. [39]:

$$\Gamma(\text{TD} \rightarrow WW/ZZ) = \delta_{W(Z)} \frac{M_{\text{TD}}^3}{8\pi F_{\text{TD}}^2} \sqrt{1 - \tau_{W/Z}} (1 - \tau_{W/Z} + \frac{3}{4} \tau_{W/Z}^2), \quad (18)$$

$$\Gamma(\text{TD} \rightarrow t\bar{t}) = \frac{3m_t^2 M_{\text{TD}}}{2\pi F_{\text{TD}}^2} (1 - \tau_t)^{3/2}, \quad (19)$$

where $\delta_{W(Z)} = 2(1)$. It is easily checked that these formulas are reduced to the SM Higgs ones just by replacing F_{TD} as $F_{\text{TD}} \rightarrow 2v_{\text{EW}}$ (We have used $(3 - \gamma_m) = 2$ in the above formulas).

The TD decay widths are thus obtained as functions of the TD mass M_{TD} , the decay constant F_{TD} and techni-fermion mass m_F in addition to the number of TC N_{TC} .

III. THE TD LHC SIGNATURES AT $\sqrt{s} = 7 \text{ TEV}$

In this section we shall discuss the TD LHC production cross sections times the branching ratios. The dominant production cross section arises through gluon fusion (GF) and vector boson fusion (VBF) processes similarly to the SM Higgs case. We thus consider these cross sections times branching ratios normalized to those of the SM Higgs:

$$R_X \equiv \frac{[\sigma_{\text{GF}}(pp \rightarrow \text{TD}) + \sigma_{\text{VBF}}(pp \rightarrow \text{TD})]}{[\sigma_{\text{GF}}(pp \rightarrow h_{\text{SM}}) + \sigma_{\text{VBF}}(pp \rightarrow h_{\text{SM}})]} \frac{BR(\text{TD} \rightarrow X)}{BR(h_{\text{SM}} \rightarrow X)}, \quad (20)$$

where $X = WW, ZZ, gg, \gamma\gamma$ and $t\bar{t}$. The ratios of the production cross sections are related to the ratios of the corresponding decay widths as [40]

$$\frac{\sigma_{\text{VBF}}(pp \rightarrow \text{TD})}{\sigma_{\text{VBF}}(pp \rightarrow h_{\text{SM}})} = \frac{\Gamma(\text{TD} \rightarrow WW)}{\Gamma(h_{\text{SM}} \rightarrow WW)} = \frac{\Gamma(\text{TD} \rightarrow ZZ)}{\Gamma(h_{\text{SM}} \rightarrow ZZ)} \equiv r_{WW/ZZ}, \quad \frac{\sigma_{\text{GF}}(pp \rightarrow \text{TD})}{\sigma_{\text{GF}}(pp \rightarrow h_{\text{SM}})} = \frac{\Gamma(\text{TD} \rightarrow gg)}{\Gamma(h_{\text{SM}} \rightarrow gg)} \equiv r_{gg}. \quad (21)$$

Hence we may rewrite Eq.(20) as

$$R_X = \left(\frac{\sigma_{\text{GF}}(pp \rightarrow h_{\text{SM}}) \cdot r_{gg} + \sigma_{\text{VBF}}(pp \rightarrow h_{\text{SM}}) \cdot r_{WW/ZZ}}{\sigma_{\text{GF}}(pp \rightarrow h_{\text{SM}}) + \sigma_{\text{VBF}}(pp \rightarrow h_{\text{SM}})} \right) r_{\text{BR}}^X, \quad (22)$$

where

$$r_{\text{BR}}^X = \frac{BR(\text{TD} \rightarrow X)}{BR(h_{\text{SM}} \rightarrow X)}. \quad (23)$$

The SM Higgs production cross sections $\sigma_{\text{GF}}(pp \rightarrow h_{\text{SM}})$ and $\sigma_{\text{VBF}}(pp \rightarrow h_{\text{SM}})$ at $\sqrt{s} = 7$ TeV are read off from Ref. [41].

For the explicit estimate of R_X in Eq.(22), we shall consider typical models of WTC (1DM and 1FM) and adopt the recent results from the LSD analysis [23] to specify the values of techni-fermion mass m_F and TD decay constant F_{TD} in such a way that the decay widths are expressed only in terms of the TD mass M_{TD} .

From Ref. [23] we read off the result on m_F obtained through the PS formula for the techni-pion decay constant F_π which is related to the EW scale v_{EW} as $v_{\text{EW}} = \sqrt{N_{\text{D}}} F_\pi$ where N_{D} denotes the number of EW doublets which equals to half of the number of techni-fermions charged under the EW gauge: $N_{\text{D}} = 1$ for 1DM and $N_{\text{D}} = 4$ for 1FM. Adding dummy techni-fermions [31] which are singlet under the EW gauge, the total number of techni-fermions N_{TF} is expressed as

$$N_{\text{TF}} = (N_{\text{TF}})_{\text{EW-singlet}} + 2N_{\text{D}}. \quad (24)$$

At the criticality where the CBZ-IRFP α_* coincides with the critical coupling α_c for the chiral symmetry breaking, the PS formula goes like

$$\frac{v_{\text{EW}}}{m_F} \simeq 0.41 \left(\frac{N_{\text{TC}}}{3} \right)^{1/2} \left(\frac{N_{\text{D}}}{1} \right)^{1/2}. \quad (25)$$

From this we have

$$\begin{aligned} m_F &\simeq 600 \text{ GeV} \left(\frac{N_{\text{TC}}}{3} \right)^{-1/2} \left(\frac{N_{\text{D}}}{1} \right)^{-1/2} \\ &\simeq \begin{cases} 735 (600) \text{ GeV} & \text{for the 1DM } (N_{\text{D}} = 1) \text{ with } N_{\text{TC}} = 2(3) \\ 367 (300) \text{ GeV} & \text{for the 1FM } (N_{\text{D}} = 4) \text{ with } N_{\text{TC}} = 2(3) \end{cases}. \end{aligned} \quad (26)$$

By using the PCDC relation, on the other hand, the TD decay constant F_{TD} and TD mass M_{TD} are related with vacuum energy V through the trace anomaly (nonperturbative scale anomaly induced by the dynamical generation of m_F) as follows:

$$F_{\text{TD}}^2 M_{\text{TD}}^2 = -d_\theta \langle \theta_\mu^\mu \rangle = -16V, \quad (27)$$

where $d_\theta (= 4)$ is the scale dimension of trace of the energy-momentum tensor θ_μ^μ . Here the vacuum energy $V = d_\theta \langle \theta_\mu^\mu \rangle / 16$ only includes contributions from the nonperturbative scale anomaly, defined by subtracting contributions $\langle \theta_\mu^\mu \rangle_{\text{perturbation}}$ of $\mathcal{O}(\Lambda_{\text{TC}}^4)$ from the perturbative running of the gauge coupling α , such as $\langle \theta_\mu^\mu \rangle - \langle \theta_\mu^\mu \rangle_{\text{perturbation}}$. To the vacuum energy V the LSD analysis in Ref. [23] gives

$$-4V \simeq 0.76 \left(\frac{N_{\text{TF}} N_{\text{TC}}}{2\pi^2} \right) m_F^4, \quad (28)$$

at the criticality, and hence

$$F_{\text{TD}}^2 M_{\text{TD}}^2 \simeq 3.0 \left(\frac{N_{\text{TF}} N_{\text{TC}}}{2\pi^2} \right) m_F^4. \quad (29)$$

This relation reflects the appropriate dependences of F_{TD} on N_{TC} and N_{TF} : F_{TD} scales with N_{TF} as well as N_{TC} like $F_{\text{TD}} \propto \sqrt{N_{\text{TC}} N_{\text{TF}}}$ [42]. Note also that the (pole) masses M_{TD} and m_F do not scale with N_{TC} and N_{TF} .

From Eq.(29) and Eq.(26) we obtain F_{TD} as a function of M_{TD} :

$$F_{\text{TD}} \simeq 1413 \text{ GeV} \left(\frac{600 \text{ GeV}}{M_{\text{TD}}} \right) \left(\frac{N_{\text{TF}}}{4N_{\text{TC}}} \right)^{1/2} \left(\frac{N_{\text{TC}}}{3} \right)^{-1/2} \left(\frac{N_{\text{D}}}{1} \right)^{-2}$$

$$\simeq \begin{cases} 1413 (1413) \text{ GeV} \left(\frac{600 \text{ GeV}}{M_{\text{TD}}} \right) & \text{for the 1DM with } N_{\text{TC}} = 2(3), N_{\text{TF}} \simeq 8(12) \\ 353 (353) \text{ GeV} \left(\frac{600 \text{ GeV}}{M_{\text{TD}}} \right) & \text{for the 1FM with } N_{\text{TC}} = 2(3), N_{\text{TF}} \simeq 8(12) \end{cases}, \quad (30)$$

where we have used $N_{\text{TF}} \simeq 4N_{\text{TC}}$ [19] obtained by estimating the critical number of flavors at which we have $\alpha_* \simeq \alpha_c$. Note that Eq.(30) merely shows the reference values of F_{TD} , not reflecting scaling properties with respect to N_{TC} and $N_{\text{D}}(N_{\text{TF}})$ because the pion decay constant $F_\pi(v_{\text{EW}}) \propto \sqrt{N_{\text{TC}}}$ has been fixed through m_F fixed as in Eq.(25).

The values of F_{TD} are somewhat larger than the pion decay constant $F_\pi \simeq 246 \text{ GeV}$ (123 GeV) for the 1DM (1FM). It turns out that the largeness of F_{TD} essentially comes from the smallness of M_{TD} tied with the existence of the approximate scale invariance: To see this more clearly, we shall go back to Eq.(29) and express m_F in terms of F_π through Eq.(26) with $v_{\text{EW}} = F_\pi/\sqrt{N_{\text{D}}}$, and then divide both sides of Eq.(29) by F_π^4 . We then arrive at

$$\frac{F_{\text{TD}}}{F_\pi} \simeq 7.0 \times \left(\frac{F_\pi}{M_{\text{TD}}} \right) \sqrt{\frac{N_{\text{TF}}}{N_{\text{TC}}}}$$

$$\simeq \begin{cases} 5.7 \left(\frac{600 \text{ GeV}}{M_{\text{TD}}} \right) & \text{for the 1DMs with } N_{\text{TF}} \simeq 4N_{\text{TC}} \text{ and } F_\pi = 246 \text{ GeV} \\ 2.8 \left(\frac{600 \text{ GeV}}{M_{\text{TD}}} \right) & \text{for the 1FMs with } N_{\text{TF}} \simeq 4N_{\text{TC}} \text{ and } F_\pi = 123 \text{ GeV} \end{cases}. \quad (31)$$

If we had $F_{\text{TD}} \sim F_\pi$, then M_{TD} would have to be $\gtrsim \mathcal{O}(\text{TeV})$ which is as large as masses of other techni-hadrons like techni-rho meson, as in the case of QCD “dilaton” such as $f_0(1370)$ (or $f_0(600)$). Thus the existence of the approximate scale invariance allowing the small M_{TD} essentially causes the large F_{TD} .

The TD Yukawa coupling to the SM fermions normalized to the SM Higgs one is estimated for each model:

$$\frac{g_{\text{TD}ff}}{g_{\text{H}ff}} = \frac{(3 - \gamma_m)v_{\text{EW}}}{F_{\text{TD}}} \Big|_{\gamma_m \simeq 1}$$

$$\simeq (3 - \gamma_m)|_{\gamma_m \simeq 1} \times \begin{cases} 0.18 \left(\frac{M_{\text{TD}}}{600 \text{ GeV}} \right) & \text{for the 1DM with } N_{\text{TF}} \simeq 4N_{\text{TC}} \\ 0.71 \left(\frac{M_{\text{TD}}}{600 \text{ GeV}} \right) & \text{for the 1FM with } N_{\text{TF}} \simeq 4N_{\text{TC}} \end{cases}. \quad (32)$$

Thus the Yukawa coupling in the 1DM gets suppressed and so do other TD couplings, mainly due to the smallness of M_{TD} as noted above. In the case of 1FM, on the other hand, its suppression is mild due to the relatively smaller F_π related to the smaller F_{TD} (See Eqs.(30) and (31)), so that the extra factor $(3 - \gamma_m) \simeq 2$ finally pulls the Yukawa coupling strength up to be comparable to the SM Higgs one. Note that were it for $M_{\text{TD}} \simeq 1.7 \text{ TeV}$ (430 GeV) in the 1DM (1FM), we would have $g_{\text{TD}ff} \simeq g_{\text{H}ff}$, which would imply that the TD signature in the 1DM then would become almost identical to those of the SM Higgs (except small corrections to the $\gamma\gamma$ mode coming from extra EM-charged techni-fermions). It is not the case, on the other hand, for the 1FM because of the presence of extra techni-quarks yielding significant contributions to the GF production cross section as will be seen below.

The TD decay widths in Eqs.(14)-(15) and (18)-(19) and the ratio r_{BR}^X in Eq.(23) are thus calculated explicitly as functions of only the TD mass M_{TD} . The comparison of the TD branching ratios with those of the SM Higgs is shown in Table I for the reference value $M_{\text{TD}} = 600 \text{ GeV}$ in the 1DM and 1FMs with $N_{\text{TC}} = 2, 3$ and the corresponding values of m_F given in Eq.(26). In the case of 1DMs the TD branching fraction becomes almost identical to that of the SM Higgs since the overall difference between the coupling strengths cancels out in the branching ratios. Also for 1FMs the same argument is applicable to the decays to WW, ZZ and $t\bar{t}$ as well, however, not to the decays to gg and $\gamma\gamma$, which are rather enhanced mainly due to the presence of extra colored (techni-quarks)/EM-charged particles contributing to these decay processes.

We next pay attention to the production cross sections. As seen from Eq.(22), the rate of the production cross section to the SM Higgs is determined by the amounts of r_{gg} and $r_{WW/ZZ}$ defined in Eq.(21) quite sensitive to the TD Yukawa couplings. The case of 1FM makes the situation most sensitive because of the presence of techni-quarks with the number of $2N_{\text{TC}}$ which in general enhances the GF cross section r_{gg} ^{#10}. For 1DMs, in contrast, it is not the

^{#10} A similar enhancement of GF process in the case of 1FM was discussed in Ref. [43].

Model	N_{TC}	r_{BR}^{WW}	r_{BR}^{ZZ}	r_{BR}^{gg}	$r_{\text{BR}}^{\gamma\gamma}$	$r_{\text{BR}}^{t\bar{t}}$
1DM	2	1.0	1.0	1.0	1.0	0.92
	3	1.0	1.0	1.0	0.80	1.0
1FM	2	1.0	0.99	16	3.2	1.0
	3	0.99	0.99	44	11	0.99

TABLE I: The TD branching ratios at $M_{\text{TD}} = 600$ GeV normalized to the corresponding quantities for the SM Higgs, r_{BR}^X ($X = WW, ZZ, gg, \gamma\gamma, t\bar{t}$), defined in Eq.(21).

Model	N_{TC}	$\frac{g_{\text{TD}ff}}{g_{h_{\text{SM}}ff}} = \frac{2v_{\text{EW}}}{F_{\text{TD}}}$	$r_{gg} = \frac{\sigma_{\text{GF}}^{\text{TD}}}{\sigma_{\text{GF}}^{h_{\text{SM}}}}$	$r_{WW/ZZ} = \frac{\sigma_{\text{VBF}}^{\text{TD}}}{\sigma_{\text{VBF}}^{h_{\text{SM}}}}$
1DM	2	0.35	0.12	0.12
	3	0.35	0.12	0.12
1FM	2	1.4	31	1.9
	3	1.4	87	1.9

TABLE II: Values of r_{gg} and $r_{WW/ZZ}$ for $N_{\text{TC}} = 2, 3$ in the case of 1FM and 1DMs with $M_{\text{TD}} = 600$ GeV fixed. Also shown are values of the ratio of the Yukawa coupling $g_{\text{TD}ff}/g_{h_{\text{SM}}ff}$.

case because of the absence of techni-quarks and the suppression of Yukawa coupling coming from somewhat larger F_{TD} sensitively reflecting the smallness of M_{TD} (See Eq.(30) and discussion below Eq.(31)).

In Table II we list the reference values of r_{gg} and $r_{WW/ZZ}$ for $M_{\text{TD}} = 600$ GeV in the case of 1DM and 1FMs with $N_{\text{TC}} = 2, 3$ together with the values of $g_{\text{TD}ff}/g_{h_{\text{SM}}ff}$ in Eq.(32). The VBF cross section in the case of 1FMs is thus almost of the same order of magnitude as that of the SM Higgs because of the almost identical Yukawa coupling strength, while the GF cross section gets highly enhanced by a factor of $\mathcal{O}(10) - \mathcal{O}(10^2)$ depending on N_{TC} due to the techni-quark contributions. For 1DMs without such an enhancement, on the other hand, both cross sections get suppressed simply due to the suppressed Yukawa couplings.

Now we calculate the value of R_X in Eq.(22) for each channel to address more clearly how we can distinguish the TD signatures from those of the SM Higgs at the LHC. The results are listed in Table III with $M_{\text{TD}} = 600$ GeV fixed.

From Table III we see that in the case of 1DMs all the signatures are suppressed to be one order of magnitude smaller than the corresponding quantities for the SM Higgs due to the large suppression of the production cross sections coming from the suppression of Yukawa coupling (See Eq.(32) or Table II). It is interesting to note, in particular, that the WW and ZZ modes get suppressed in contrast to the SM Higgs case, to be distinguishable from those of the SM Higgs at the LHC.

In the case of 1FMs, on the other hand, all the signals get enhanced due to the large GF production cross section highly enhanced by the extra colored-techni-quark contributions (See Table II). This enhancement gets more operative for the gg and $\gamma\gamma$ modes to result in a gigantic enhancement mainly because of their highly enhanced branching ratios (See Table I). Note that the LHC cross section for the $\gamma\gamma$ mode is quite small for the SM Higgs with the mass around 600 GeV, which is about $10^{-4} - 10^{-3}$ fb. Besides the enhanced WW and ZZ modes, therefore, the $\gamma\gamma$ mode will be a characteristic signature of TD clearly distinguishable from the SM Higgs to be visible at the LHC, as will explicitly be shown below. The enhancement in the $t\bar{t}$ mode may also be a certain TD signature (See the discussion in the last section), while the gg mode is inaccessible for the TD searches because of its huge background.

We now check the consistency of the TD signatures with the recent data at the LHC accumulated by the ATLAS

Model	N_{TC}	R_{WW}	R_{ZZ}	R_{gg}	$R_{\gamma\gamma}$	$R_{t\bar{t}}$
1DM	2	0.12	0.12	0.12	0.095	0.12
	3	0.12	0.12	0.12	0.097	0.12
1FM	2	26	26	414	85	26
	3	73	73	3300	840	73

TABLE III: The TD signatures at $M_{\text{TD}} = 600$ GeV normalized to the corresponding quantities for the SM Higgs, R_X ($X = WW, ZZ, gg, \gamma\gamma, t\bar{t}$) defined in Eq.(22).

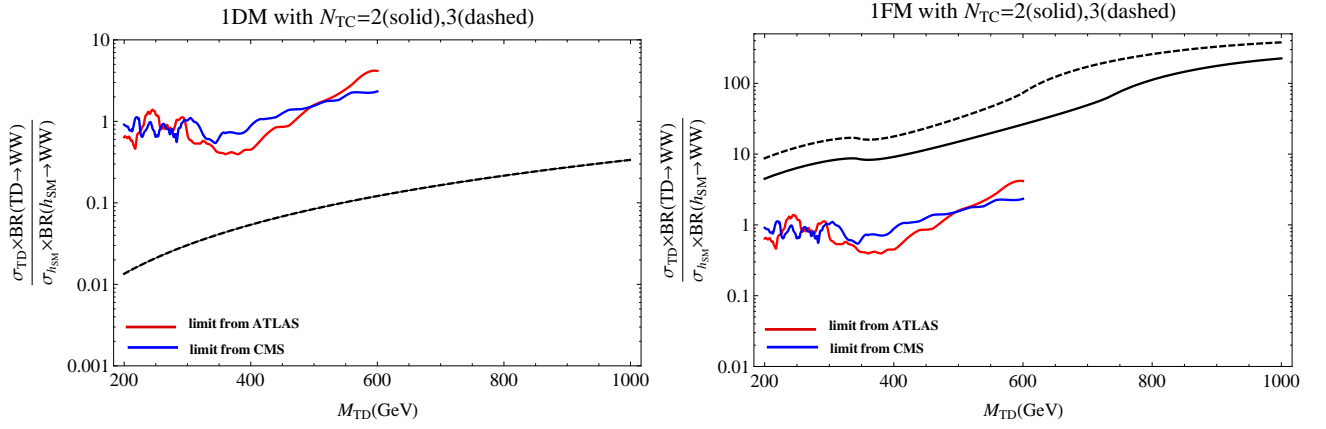


FIG. 3: Left panel: The TD LHC production cross sections at $\sqrt{s} = 7$ TeV times the WW/ZZ branching ratio in the 1DMs with $N_{TC} = 2, 3$ normalized to the corresponding quantity for the SM Higgs. Also shown is the comparison with the 95% C.L. upper limits from the ATLAS [1] and CMS [2]. Right panel: The same as the left panel for the 1FMs.

and CMS detectors [1, 2]. Varying the TD mass in the range $200 \text{ GeV} < M_{TD} < 1000 \text{ GeV}$, in Fig. 3 we plot the TD LHC production cross sections at $\sqrt{s} = 7$ TeV times the WW branching ratio (R_{WW} in Eq.(22)) normalized to the corresponding quantity for the SM Higgs. The red and blue curves stand for the 95% C.L. upper limits from the ATLAS and CMS experiments, respectively. Looking at Fig. 3, we see that in the case of 1DMs the TD signature is consistent with the current experimental data over all the mass range $200 \text{ GeV} < M_{TD} < 600 \text{ GeV}$ thanks to the large suppression of GF cross section, which on the other side of the coin would imply that the TD may be invisible through this channel in contrast to the SM Higgs. For the 1FMs, on the other hand, the consistency with the experimental data requires the TD mass to be $M_{TD} \gtrsim 600 \text{ GeV}$, which conversely would imply that the TD can be discovered through somewhat large excesses at $600 \text{ GeV} \lesssim M_{TD} < 1000 \text{ GeV}$ in this channel in the near future.

Since the $\gamma\gamma$ mode in the 1FMs get highly enhanced in contrast to the SM Higgs case as seen from Table III, in Fig. 4 we finally plot the TD LHC production cross section at $\sqrt{s} = 7$ TeV times the $\gamma\gamma$ branching ratio in the case of 1FMs over the TD mass range $200 \text{ GeV} < M_{TD} < 1000 \text{ GeV}$. The figure tells us that the cross sections are large enough to be comparable with the golden mode of SM Higgs signature $pp \rightarrow h_{SM} \rightarrow ZZ \rightarrow l^+l^-l^+l^- \sim 1 \text{ fb}$ around the SM Higgs mass $\simeq 600 \text{ GeV}$: At around $M_{TD} \simeq 600 \text{ GeV}$, indeed, we have

$$\sigma_{TD} \times BR(TD \rightarrow \gamma\gamma) \Big|_{1FM} \sim 0.10 (1.0) \text{ fb}, \quad \text{for} \quad N_{TC} = 2(3). \quad (33)$$

This implies that the TD can be discovered through the $\gamma\gamma$ channel at the upcoming several months.

IV. SUMMARY AND DISCUSSION

In this paper we have studied the LHC signatures of TD arising as a composite pNGB of the spontaneous and explicit breaking of the scale symmetry in WTC. The TD couplings to the SM particles were obtained, based on the nonlinear realization of the electroweak symmetry as well as the scale symmetry (via spurion method) which is broken not only spontaneously but also explicitly by the very origin of the spontaneous breaking, i.e., the dynamical generation of the techni-fermion mass (nonperturbative scale anomaly). As a result, the TD couplings are similar to those of the SM Higgs except the overall scale set by the TD decay constant (and the anomalous dimension) instead of the EW scale.

We took typical models of WTC such as 1DM and 1FM to make an explicit estimate of the branching ratios and production cross sections. To be more concrete, we further adopted the results from the recent LSD analysis combined with the PCDC relation to get the TD couplings as functions of the TD mass only.

We calculated the TD decay widths and branching ratios to find that in the case of 1DMs the branching fraction becomes almost identical to that of the SM Higgs because of the similar form (though suppressed) of the TD coupling (See Eq.(32)). While in the 1FMs the branching ratios of $TD \rightarrow gg$ and $\gamma\gamma$ get highly enhanced due to presence of the extra contributions of techni-quarks (See Table I). The same mechanism is effective also in the production cross sections: For 1DMs both the GF and VBF cross sections are suppressed compared to the SM Higgs case due to

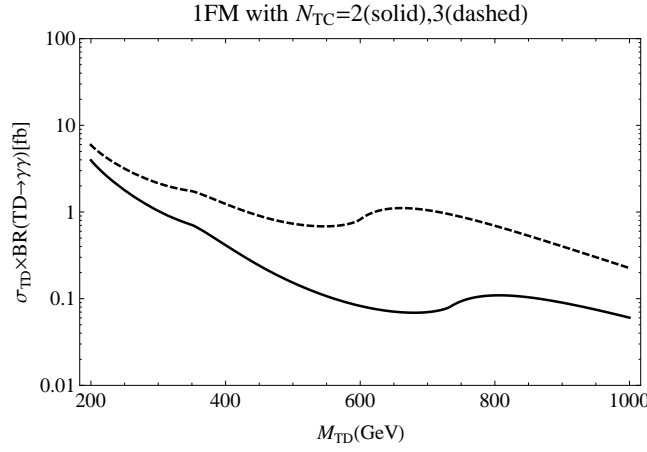


FIG. 4: The TD LHC production cross section at $\sqrt{s} = 7$ TeV times the $\gamma\gamma$ branching ratio in unit of fb for the 1FMs with $N_{TC} = 2, 3$.

the suppression of TD couplings, while for 1FMs they get larger, where the amount of enhancement becomes more outstanding for the GF production (See Table II).

The TD LHC signatures were then discussed by explicitly calculating the production cross sections times the branching ratios in comparison with the corresponding quantities for the SM Higgs. It turned out that the TD signatures look like quite different from the corresponding SM Higgs signatures: For 1DMs, all the TD signatures become one order of magnitude down compared with those of the SM Higgs, which would imply that if the Higgs-like object was found in the region above 600 GeV, it would be naturally interpreted as TD, since the SM Higgs unlikely has such a large mass. On the other hand, for 1FMs all those signatures were shown to be enhanced by a factor of $\mathcal{O}(10) - \mathcal{O}(10^2)$ and would become outstanding signals of TD (See Table III).

Varying the TD mass in the range $200 \text{ GeV} < M_{TD} < 1000 \text{ GeV}$, the cross section $pp \rightarrow TD \rightarrow WW$ per the corresponding quantity for the SM Higgs has been compared with the recent upper limits from the ATLAS and CMS experiments. In the case of 1DMs the TD signature is consistent with the current experimental data over the mass range $200 \text{ GeV} < M_{TD} < 600 \text{ GeV}$ thanks to the large suppression of GF cross section, though the TD may be invisible through this channel in contrast to the SM Higgs. For the 1FMs, on the other hand, the signals enhanced over the whole mass range are severely constrained and the consistency with the experimental data requires the TD mass to be $M_{TD} > 600 \text{ GeV}$, which, however, would also imply that the TD might be discovered through somewhat large excesses at $600 \text{ GeV} \lesssim M_{TD} < 1000 \text{ GeV}$ in this channel in the near future (See Fig. 3).

Furthermore, the cross section $pp \rightarrow TD \rightarrow \gamma\gamma$ for the 1FMs was predicted to be $\sim 0.10 - 1.0 \text{ fb}$ for the TD mass around 600 GeV (See Fig. 4 and Eq.(33)). This cross section is large enough for the TD to be discovered in the upcoming several months and hence will also be a characteristic signature of TD.

Before closing this section, several comments are in order:

TD LHC signature from the $t\bar{t}$ mode — First of all, it is worth commenting on the TD LHC signature through the decay to $t\bar{t}$. The ATLAS at $\sqrt{s} = 7$ TeV with the integrated luminosity of 0.7 fb^{-1} has already measured the $t\bar{t}$ production cross section $\sigma_{t\bar{t}}$ to report that $\sigma_{t\bar{t}} = 179.0 \pm 11.8 \text{ pb}$ [44], in agreement with the SM prediction. The SM Higgs contribution to this cross section is estimated to be about 0.1 pb at around the mass $\simeq 600 \text{ GeV}$ and hence is negligible in comparison with the dominant QCD contributions incorporated in the SM estimate of $\sigma_{t\bar{t}}$. As seen from Table III, on the other hand, the cross section $\sigma(pp \rightarrow TD \rightarrow t\bar{t})$ in the case of 1FMs gets enhanced by a factor of about 30 (70) for $N_{TC} = 2(3)$ with $M_{TD} = 600 \text{ GeV}$ compared to the SM Higgs case, so we would have $\sigma(pp \rightarrow TD \rightarrow t\bar{t}) \simeq 3(7) \text{ pb}$. Thus this signature is currently just as much as the size of the measurement uncertainties, but would be testable if more precise measurement of $\sigma_{t\bar{t}}$ becomes possible in the future.

Perturbative unitarity — For the 1FMs we might put an upper limit on M_{TD} coming from the perturbative unitarity bound through a formula, $M_{TD} \lesssim \Lambda_{\text{uni}} = \sqrt{8\pi} F_\pi = \sqrt{8\pi} \cdot \left(\frac{246 \text{ GeV}}{\sqrt{N_D}} \right)$ [45]. By this formula we get $\Lambda_{\text{uni}} \simeq 617 \text{ GeV}$ for the 1FMs, while it is absent for the 1DMs because the bound is estimated to be above 1 TeV. Looking at Figs. 3 and 4 with this unitarity bound taken into account, one might think that the 1FMs have completely been ruled out (up to the narrow window $600 \text{ GeV} < M_{TD} < 617 \text{ GeV}$). Note however that the perturbative unitarity

bound is thought of as just a reference, which may not make much sense, since WTC is itself of course unitary and the low-energy effective theory is still strongly coupled and not perturbative.

Comparison with other dilaton phenomenology [46] — Another approach on a dilaton signature at the LHC has been addressed in Ref. [46]. Their dilaton is, however, completely different from our TD in the sense that theirs' is not due to the scale symmetry of the WTC but the whole system including SM and the underlying EW theory (possibly including the WTC). Thus the characteristic feature is completely different from ours.

Non-running coupling case — In this paper we employed LSD calculation of the nonperturbative scale anomaly via vacuum energy, using the two-loop running coupling with CBZ-IRFP in Ref. [23]. We here discuss the comparison with the non-running limit. In this limit the very origin of the dynamical mass m_F comes from the cutoff Λ , the relation (hierarchy) between the two being given in the characteristic form of essential singularity (Miransky scaling) [8]:

$$m_F \sim \Lambda \cdot \exp\left(-\frac{\pi}{\sqrt{\frac{\alpha}{\alpha_c} - 1}}\right) \ll \Lambda \quad (\alpha \searrow \alpha_c) . \quad (34)$$

The coupling α should depend on Λ/m_F in such a way that $\alpha(\Lambda/m_F) \rightarrow \alpha_c$ in the limit $\Lambda/m_F \rightarrow \infty$, resultant beta function being $\beta(\alpha) = \Lambda \partial\alpha/\partial\Lambda = -(2\alpha_c/\pi)(\alpha/\alpha_c - 1)^{3/2}$. Hence the cutoff cannot be removed without requiring *nonperturbative running* of the coupling: The coupling (non-running in the perturbative sense) does actually run slowly (walking) towards the critical coupling (regarded as the ultraviolet (UV) fixed point) at $\Lambda/m_F \rightarrow \infty$, reflecting the scale anomaly, i.e., explicit breaking of the scale symmetry (See Figs. 1(a) and (b) in the first of Ref. [5] for the beta function (a) and the associated anomalous dimension (b)).

Now in the WTC model based on the two-loop coupling with CBZ-IRFP, the role of the cutoff Λ in the non-running case of the original WTC model [5, 6] is simply traded for the intrinsic scale $\Lambda_{\text{TC}} (\gg m_F)$ of the two-loop coupling, which breaks the scale symmetry already at perturbative level for the UV region ($p > \Lambda_{\text{TC}}$) where the coupling runs as $1/\ln p$ as in the ordinary QCD. Although in the IR region ($p < \Lambda_{\text{TC}}$) the coupling governed by CBZ-IRFP is almost non-running (scale invariant/conformal), the scale symmetry is broken both spontaneously and explicitly by yet another dynamics, namely the dynamical generation of the techni-fermion mass $m_F (\ll \Lambda_{\text{TC}})$, and the coupling does run according to the nonperturbative renormalization a la Miransky in much the same way as the nonperturbative running of the non-running coupling case mentioned above. It was argued [15] that for the dynamical mass generation of essential singularity type scaling Eq.(34), characterized as “conformal phase transition”, the associated nonperturbative scale anomaly (explicit breaking of the scale symmetry) is saturated by the pseudo dilaton (“massive dilaton”) which are dictated by the PCDC.

Although the analysis of Ref. [23] was done for the case $\Lambda_{\text{ETC}} \simeq \Lambda_{\text{TC}}$, we may take a choice $\Lambda_{\text{ETC}} \ll \Lambda_{\text{TC}}$, in which case the WTC would simply be reduced to the original WTC model of Ref. [5, 6] where the two-loop perturbative coupling becomes essentially scale invariant (non-running) all the way up to $\Lambda = \Lambda_{\text{ETC}}$ ^{#11}. In such a case the estimate of the scale anomaly through the vacuum energy was done long time ago [16] which differs from Eq.(27) only by the factor 0.81 in place of 0.76. Thus our estimate in the text would be qualitatively the same as it stands: In fact, the estimated values of m_F and F_{TD} in Eqs.(26) and (30) will be shifted upward only by about 5% in the case of the non-running coupling. This happens because of about 5% reduction and enhancement of the overall numerical coefficients in Eqs.(25) and (29), respectively: $0.41 \rightarrow 0.39$ in Eq.(25), while $3.0 \rightarrow 3.2$ in Eq.(29). The Yukawa couplings will then get smaller than those listed in Table II by a factor of about 17%, so the GF cross sections will be reduced by about 30% at around $M_{\text{TD}} = 600$ GeV. The amount of TD LHC signatures will thus be reduced only by about 30% compared to those predicted in Figs. 3 and 4 and will not substantially change.

^{#11} In this case WTC dynamics in isolation does not make sense in the asymptotically-free region $p > \Lambda_{\text{TC}} (\gg \Lambda_{\text{ETC}})$, since then the theory will be changed already at lower scale Λ_{ETC} into a different theory, ETC (or the preon model where SM particles and techni-fermions are the composites on the same footing [47]).

Acknowledgments

We would like to thank T. Abe and M. Hashimoto for useful comments and discussions. This work was supported by the JSPS Grant-in-Aid for Scientific Research (S) #22224003 and (C) #23540300 (K.Y.).

-
- [1] ATLAS Collaboration, “Update of the Combination of Higgs Boson Searches in 1.0 to 2.3 fb⁻¹ of pp Collisions Data Taken at $\sqrt{s} = 7$ TeV with the ATLAS Experiments at the LHC,” ATLAS-CONF-2011-135, 22 August 2011.
 - [2] CMS Collaboration, “Search for standard model Higgs boson in pp collisions at $\sqrt{s} = 7$ TeV and integrated luminosity up to 1.7 fb⁻¹,” CMS PAS HIG-11-022, August 22, 2011.
 - [3] For reviews, see, e.g., E. Farhi and L. Susskind, Phys. Rept. **74**, 277 (1981); K. Yamawaki, Lecture at 14th Symposium on Theoretical Physics, Cheju, Korea, July 1995, arXiv:hep-ph/9603293; C. T. Hill and E. H. Simmons, Phys. Rept. **381**, 235 (2003) [Erratum-ibid. **390**, 553 (2004)]; F. Sannino, Acta Phys. Polon. **B40**, 3533-3743 (2009).
 - [4] S. Weinberg, Phys. Rev. D **13**, 974 (1976); L. Susskind, Phys. Rev. D **20**, 2619 (1979).
 - [5] K. Yamawaki, M. Bando and K. Matumoto, Phys. Rev. Lett. **56**, 1335 (1986); M. Bando, T. Morozumi, H. So and K. Yamawaki, Phys. Rev. Lett. **59**, 389 (1987).
 - [6] M. Bando, K. Matumoto and K. Yamawaki, Phys. Lett. B **178**, 308 (1986).
 - [7] B. Holdom, Phys. Rev. D **24**, 1441 (1981).
 - [8] V. A. Miransky, Nuovo Cim. A **90**, 149 (1985).
 - [9] T. Akiba and T. Yanagida, Phys. Lett. B **169**, 432 (1986); T. W. Appelquist, D. Karabali and L. C. R. Wijewardhana, Phys. Rev. Lett. **57**, 957 (1986); T. Appelquist and L. C. R. Wijewardhana, Phys. Rev. D **36**, 568 (1987). Work without concept of anomalous dimension was also done earlier, based on the pure numerical analysis, see B. Holdom, Phys. Lett. B **150**, 301 (1985).
 - [10] T. Appelquist and G. Triantaphyllou, Phys. Lett. B **278**, 345 (1992); R. Sundrum and S. D. H. Hsu, Nucl. Phys. B **391**, 127 (1993); T. Appelquist and F. Sannino, Phys. Rev. D **59**, 067702 (1999).
 - [11] M. Harada, M. Kurachi and K. Yamawaki, Prog. Theor. Phys. **115**, 765 (2006); M. Kurachi and R. Shrock, Phys. Rev. D **74**, 056003 (2006); M. Kurachi, R. Shrock and K. Yamawaki, Phys. Rev. D **76**, 035003 (2007).
 - [12] S. Dimopoulos and L. Susskind, Nucl. Phys. B **155**, 237 (1979); E. Eichten and K. D. Lane, Phys. Lett. B **90**, 125 (1980).
 - [13] G. Cacciapaglia, C. Csaki, C. Grojean and J. Terning, Phys. Rev. D **71**, 035015 (2005); R. Foadi, S. Gopalakrishna and C. Schmidt, Phys. Lett. B **606**, 157 (2005); R. S. Chivukula, E. H. Simmons, H. J. He, M. Kurachi and M. Tanabashi, Phys. Rev. D **72**, 015008 (2005).
 - [14] D. Black, A. H. Fariborz and J. Schechter, Phys. Rev. D **61**, 074001 (2000); G. 't Hooft, G. Isidori, L. Maiani, A. D. Polosa and V. Riquer, Phys. Lett. B **662**, 424 (2008).
 - [15] V. A. Miransky and K. Yamawaki, Phys. Rev. D **55**, 5051 (1997); Errata, **56**, 3768 (1997).
 - [16] V. A. Miransky and V. P. Gusynin, Prog. Theor. Phys. **81**, 426 (1989).
 - [17] W. A. Bardeen, C. N. Leung and S. T. Love, Phys. Rev. Lett. **56**, 1230 (1986); ; C. N. Leung, S. T. Love and W. A. Bardeen, Nucl. Phys. B **323**, 493 (1989); B. Holdom and J. Terning, Phys. Lett. B **187**, 357 (1987); Phys. Lett. B **200**, 338 (1988); K. i. Kondo, H. Mino and K. Yamawaki, Phys. Rev. D **39**, 2430 (1989); K. Yamawaki, in *Proc. Johns Hopkins Workshop on Current Problems in Particle Theory 12, Baltimore, June 8-10, 1988*, edited by G. Domokos and S. Kovesi-Domokos (World Scientific Pub. Co., Singapore 1988); T. Nonoyama, T. B. Suzuki and K. Yamawaki, Prog. Theor. Phys. **81**, 1238 (1989).
 - [18] K. D. Lane and M. V. Ramana, Phys. Rev. D **44**, 2678 (1991).
 - [19] T. Appelquist, J. Terning and L. C. Wijewardhana, Phys. Rev. Lett. **77**, 1214 (1996); T. Appelquist, A. Ratnaweera, J. Terning and L. C. Wijewardhana, Phys. Rev. D **58**, 105017 (1998).
 - [20] W. E. Caswell, Phys. Rev. Lett. **33**, 244 (1974); T. Banks and A. Zaks, Nucl. Phys. B **196**, 189 (1982).
 - [21] K. Yamawaki, Prog. Theor. Phys. Suppl. **180**, 1 (2010) [arXiv:0907.5277 [hep-ph]]; Int. J. Mod. Phys. A **25**, 5128 (2010) [arXiv:1008.1834 [hep-ph]].
 - [22] L. Vecchi, JHEP **1104**, 127 (2011).
 - [23] M. Hashimoto and K. Yamawaki, Phys. Rev. D **83**, 015008 (2011).
 - [24] T. Appelquist and Y. Bai, Phys. Rev. D **82**, 071701 (2010). See also D. D. Dietrich, F. Sannino and K. Tuominen, Phys. Rev. D **72**, 055001 (2005).
 - [25] K. Haba, S. Matsuzaki, K. Yamawaki, Phys. Rev. D **82**, 055007 (2010).
 - [26] K. Y. Choi, D. K. Hong and S. Matsuzaki, arXiv:1101.5326 [hep-ph].
 - [27] S. Shuto, M. Tanabashi and K. Yamawaki, in *Proc. 1989 Workshop on Dynamical Symmetry Breaking*, Dec. 21-23, 1989, Nagoya, eds. T. Muta and K. Yamawaki (Nagoya Univ., Nagoya, 1990) 115-123; M. S. Carena and C. E. M. Wagner, Phys. Lett. B **285**, 277 (1992); M. Hashimoto, Phys. Lett. B **441**, 389 (1998).
 - [28] M. Harada, M. Kurachi and K. Yamawaki, Phys. Rev. D **68**, 076001 (2003); M. Kurachi and R. Shrock, JHEP **0612**, 034 (2006).
 - [29] D. Kutasov, J. Lin and A. Parnachev, arXiv:1107.2324 [hep-th].
 - [30] M. E. Peskin and J. D. Wells, Phys. Rev. D **64**, 093003 (2001).
 - [31] N. D. Christensen and R. Shrock, Phys. Lett. B **632**, 92 (2006); M. A. Luty, JHEP **0904**, 050 (2009).

- [32] J. Gasser and H. Leutwyler, *Annals Phys.* **158**, 142 (1984); *Nucl. Phys. B* **250**, 465 (1985).
- [33] H. Pagels and S. Stokar, *Phys. Rev. D* **20**, 2947 (1979).
- [34] V. A. Miransky, M. Tanabashi and K. Yamawaki, *Phys. Lett. B* **221**, 177 (1989); *Mod. Phys. Lett. A* **4**, 1043 (1989); Y. Nambu, Enrico Fermi Institute Report No. 89-08, 1989; W. J. Marciano, *Phys. Rev. Lett.* **62** (1989), 2793; *Phys. Rev. D* **41** (1990), 219; W. A. Bardeen, C. T. Hill and M. Lindner, *Phys. Rev. D* **41** (1990), 1647.
- [35] V. A. Miransky, K. Yamawaki, *Mod. Phys. Lett. A* **4**, 129-135 (1989).
- [36] K. Matumoto, *Prog. Theor. Phys.* **81**, 277-279 (1989); T. Appelquist, M. Einhorn, T. Takeuchi, L. C. R. Wijewardhana, *Phys. Lett. B* **220**, 223 (1989).
- [37] T. E. Clark, C. N. Leung and S. T. Love, *Phys. Rev. D* **35**, 997 (1987).
- [38] M. Hashimoto, arXiv:1109.2554 [hep-ph].
- [39] M. Spira, *Fortsch. Phys.* **46**, 203 (1998) [arXiv:hep-ph/9705337].
- [40] H. M. Georgi, S. L. Glashow, M. E. Machacek, D. V. Nanopoulos, *Phys. Rev. Lett.* **40**, 692 (1978).
- [41] LHC Higgs Cross Section Working Group, updated May 25, 2011, <https://twiki.cern.ch/twiki/bin/view/LHCPhysics/CERNYellowReportPageAt7TeV>.
- [42] V. P. Gusynin, V. A. Miransky, *Phys. Lett. B* **198**, 79-83 (1987).
- [43] M. Hashimoto, *Phys. Rev. D* **83**, 096003 (2011).
- [44] ATLAS Collaboration, “Measurement of the $t\bar{t}$ production cross-section in pp collisions at $\sqrt{s} = 7$ TeV using kinematic information of lepton + jets events,” ATLAS-CONF-2011-121, 21 August 2011.
- [45] B. W. Lee, C. Quigg and H. B. Thacker, *Phys. Rev. Lett.* **38**, 883 (1977).
- [46] W. D. Goldberger, B. Grinstein and W. Skiba, *Phys. Rev. Lett.* **100**, 111802 (2008); J. Fan, W. D. Goldberger, A. Ross and W. Skiba, *Phys. Rev. D* **79**, 035017 (2009).
- [47] K. Yamawaki and T. Yokota, *Phys. Lett. B* **113**, 293 (1982).